ACOUSTICS 2012

What can we learn about the wolf phenomenon from a linearized analysis?

V. Debut[a], J. Antunes[a] and O. Inacio[b]

[a]Instituto Tecnologico e Nuclear, Estrada Nacional 10, 2686 Sacavem, Portugal
[b]Instituto Politecnico do Porto, Escola Superior de Musica e Artes do Espectaculo, IPP/ESMAE Rua da Alegria 503, 4000 Porto, Portugal
vincentdebut@itn.pt

String players, and especially cellists, are well aware of a perverse phenomenon known as wolf notes. Physically, such undesirable effect results from a severe interaction between the string and body vibrations, which are coupled at the bridge, when the sounding note approaches the frequency of a low-damped body mode. The phenomenon has invested considerable efforts to deal with the string/body coupled system. Particularly, different approaches have been adopted to achieve nonlinear time-domain simulations, including methods based on wave propagation and reflections as well as modal methods used by the present authors. Recently, the modal-based modelling developed initially by the authors has been used to address the linearized modal dynamics of the bowed string/body coupled system. Interestingly, the stability analysis provides a range of instability for a pair of coupled modes as the playing frequency approaches that of the instrument body, suggesting that the basic mechanism of the wolf phenomenon can be explained by a linear approach. Here, on the basis of our previous studies, we examine the features of the linearized modal dynamics of the bowed string/body coupled model. The influence of parametric changes in the control parameters is explored providing the modal frequency and modal damping values as a function of the bowing parameters. Particularly, results show the dependence of the wolf beating frequency on the control parameters as attested by the evidence of both experiments and nonlinear computations.

1 Introduction

Wolf note phenomenon in bowed-string instruments has been the subject of various studies whether to prove of our understanding of the complex dynamical behaviour displayed by bowed string instruments or to provide guidelines for instrumentalists to control such undesirable phenomenon. When a wolf note occurs, a low-frequency beating pervades the instrument response resulting in a characteristic warbling sound and leading to a difficult control of the played note. Physically, the origin of the wolf note problem is a coupling phenomenon resulting from the proximity of a string bowed note and the modal frequency of a low-damped mode of the instrument body.

The question of an instrument's susceptibility to wolf behaviour was first discussed by Schelleng [1]. Using a frequency approach, Schelleng proposed a quantitative criterion for the appearance of wolf-notes in terms of the string-to-body impedance ratio and of the quality factor of the body resonance responsible for the wolf. Later, using bow-force limits arguments, Woodhouse [2] derived a quite different criterion of wolf susceptibility involving a condition on the bowing contact point as evoked by Gough's observations [3]. Apart from such theoretical approaches, the wolf-note phenomenon has also been studied by computer simulations, first in the manner proposed by McIntyre, Schumacher and Woodhouse [4, 5]. An interesting situation is revealed when the normal bow force is changed: pressing harder with the bow tends to slow down the beating in the wolf note before suppressing it, a phenomenon previously observed by Raman [6]. In a recent paper, Inacio et al. [7] successfully achieved numerical simulations pertaining to wolf notes using a modal-based approach. Their simulations clearly illustrated the fact that the wolf note beating frequency changes for different playing conditions, pointing out the crucial role of the nonlinear feedback in determining wolf note essential characteristics.

Although studies on the wolf note became less fashionable, it appears that there are still few aspects deserving exploration. The purpose of this work is to illustrate that a linearized approach of the bowed string as proposed in [8] can be instructive in exploring the wolf note phenomenon in several of its characteristics. Recently, a first attempt has been presented by the authors considering a linearized formulation of the string/body coupled system and performing an eigenvalue analysis. Results provide a region of instability for a pair of coupled modes - which might be responsible for the wolf - as the playing frequency approaches that of the instrument body [9]. Overall, it suggests that if the underlying basic mechanism of wolf phenomenon may actually be explained by a linear model, other aspects may also be analysed using such simple model.

In this paper, we consider a linearized approach for the bowed string/body coupled system based on a modal representation of the system dynamics as presented in [9]. We explore the model to interpret the dependence of the wolf beating frequencies with the control parameters and compare the linear predictions with the corresponding nonlinear time-domain simulations. The paper starts with a brief recall of our approach for achieving time-domain numerical simulations for the string/body coupled system subjected to the highly nonlinear bow/string friction excitation mechanism. A few demonstrative simulations of wolves are then presented, focusing on the self-excited responses of the system for normal bow force and bow velocity ramps. The modal equations of the string/body coupled system are then linearized in the vicinity of a steady sliding state enabling the computation of the system eigenproperties. It provides insights into the changes in modal frequencies and modal damping of the coupled system in relation to the control parameters. Results show that the frequency dependence of the beating frequency observed in the nonlinear computations can be understood by such simple model. Although not all the complex dynamics of the bowed string can be explained by this kind of linear view, the paper shows that performing a linear analysis can be instructive to interpret nonlinear regimes, at least qualitatively and for low-computational costs.

2 Nonlinear time-domain simulations of the string/body coupled system

The modal-based computational approach used here has already proved its efficiency in previous works concerning bowed musical instruments. Details can be found in [7, 9].

2.1 Computational model

2.1.1 Formulation of the string dynamics

We consider an ideal string of length L , cross-sectional area S and density ρ, fixed at both ends and stretched to an axial tension T. The small-amplitude transverse displacement $y_s(x,t)$ of a conservative string subjected to the ex-

ternally applied excitation $f(x,t)$ is described by the classic wave equation:

$$\rho S \frac{\partial^2 y_s}{\partial t^2} - T \frac{\partial^2 y_s}{\partial x^2} = f(x,t) \quad (1)$$

Adopting a modal formulation in terms of the string unconstrained real modes, Eq.(1) becomes:

$$[\mathbf{M_s}]\{\ddot{Q}_s\} + [\mathbf{C_s}]\{\dot{Q}_s\} + [\mathbf{K_s}]\{Q_s\} = \{F(t)\} \quad (2)$$

where dissipation in the form of modal damping was introduced. $[\mathbf{M_s}]$, $[\mathbf{C_s}]$ and $[\mathbf{K_s}]$ are diagonal matrices of the string modal parameters $m_n = \rho S L/2$, $c_n = 2m_n\omega_n\zeta_n$ and $k_n = m_n\omega_n^2$, with ω_n the circular eigenfrequencies, ζ_n the damping values and $n = 1, \ldots, N_s$ the mode index. $\{Q_s(t)\} = \{q_1(t), \ldots, q_{N_s}(t)\}^T$ is the vector of the modal responses and $\{F(t)\} = \{\mathcal{F}_1(t), \ldots, \mathcal{F}_{N_s}(t)\}^T$ is the vector of the modal forces obtained by projecting the external forces on the string modeshapes $\varphi_n(x) = \sin(n\pi x/L)$:

$$\mathcal{F}_n(t) = \int_0^L f(x,t)\varphi_n(x)\, dx \quad (3)$$

In the following, the external force field is due to the localized forces namely: (1) the friction force exerted by the bow on the string, (2) the interaction force between the string and the instrument body, and (3) the possible presence of a finger on the fingerboard. The physical motion at any point of the string can be computed from the modal amplitudes $q_n(t)$ by superposition:

$$y_s(x,t) = \sum_{n=1}^{N_s} q_n(t)\varphi_n(x) \quad (4)$$

2.1.2 The friction model

The friction model used in the numerical simulations is of the Coulomb type with a velocity-dependent friction coefficient. The friction force $f_c(t)$ arising between the string and the bow at the contact location x_c is given by

$$\begin{cases} f_c(t) = -\mu_d(v_c)\, F_N\, \text{sign}(v_c) & \text{if} \quad |v_c(t)| > 0 \\ f_c(t) \leq -\mu_S\, F_N & \text{if} \quad |v_c(t)| = 0 \end{cases} \quad (5)$$

where F_N is the normal force between the bow and the string, μ_S is a static friction coefficient during surface adherence and $v_c(t) = \dot{y}_s(x_c,t) - v_b(t)$ is the relative velocity between the string surface and the driving bow. The dynamic friction coefficient $\mu_d(v_c)$ used during sliding depends on the relative bow-string velocity according to:

$$\mu_d(v_c) = \mu_D + (\mu_S - \mu_D)e^{-C|v_c|} \quad (6)$$

where μ_D is an asymptotic limit of the friction coefficient when $|v_c| \to \infty$ and C is a parameter controlling the decay rate of the friction coefficient with $v_c(t)$. The friction model (6) can be readily fitted to typical experimental data by adjusting the empirical constants μ_S, μ_D and C. Basically, sticking is simulated using an adherence stiffness as detailed in [7, 9].

2.1.3 Formulation of the body dynamics

The response of the body can be represented by a simplified modal model:

$$[\mathbf{M_b}]\{\ddot{Q}_b\} + [\mathbf{C_b}]\{\dot{Q}_b\} + [\mathbf{K_b}]\{Q_b\} = \{F_b(t)\} \quad (7)$$

where $[\mathbf{M_b}]$, $[\mathbf{C_b}]$ and $[\mathbf{K_b}]$ are diagonal matrices for the instrument body modal parameters, $\{Q_b(t)\} = \{q_1(t), \ldots, q_{M_b}(t)\}^T$ and $\{F_b(t)\} = \{\mathcal{F}_1(t), \ldots, \mathcal{F}_{M_b}(t)\}^T$ are the vectors for the body modal responses and generalized forces respectively. The modal forces are obtained by projecting the bridge/body interaction force on the instrument body modal basis. The body modal parameters were identified from a single transfer function measurement at the bridge using the ERA algorithm [10, 11]. The cello modeshapes were assumed real and the modal masses were computed by postulating that the corresponding modeshapes are unitary at the bridge location.

2.1.4 String/body coupling

Coupling between the string and the body is achieved using a penalty formulation, by connecting the string to the bridge through a very stiff spring. The force $f_b(x_b,t)$ exterted by the body on the string at the bridge location x_b is:

$$f_b(x_b,t) = -K_{BS}\,[y_s(x_b,t) - y_b(x_b,t)] \quad (8)$$

where K_{BS} is an empirical stiffness coefficient.

2.1.5 Finger control of the playing frequency

In order to control the playing frequency and shorten the active length of the string, an artifical finger was modelled using three spring/dashpots at coordinates $x_{f_1} = x_f - W_f/2$, $x_{f_2} = x_f$ and $x_{f_3} = x_f + W_f/2$ where x_f and W_f are the location and width of the finger respectively. As for the string/body coupling, the interaction force $f_{f_j}(x_j,t)$ exerted by the finger on the string at location x_j is modelled using a penalty formulation, imposing a near-zero displacement according to:

$$f_{f_j}(x_j,t) = -K_{FS}\, y_s(x_{f_j},t) - C_{FS}\, \dot{y}_s(x_{f_j},t) \qquad (j = 1,2,3) \quad (9)$$

where K_{FS} and C_{FS} are the empirical stiffness and damping coupling coefficients.

2.2 Numerical simulations

The method previously described was used to simulate the time-domain dynamical responses of the string/body coupled system. Calculations were made for a cello string with a linear density of $\rho = 14 \times 10^{-3}$ kg.m^{-1} and a total length $L =$ 0.83 m from the tailpiece to the nut, with an active length of 0.7 m from the bridge to the nut. The fundamental frequency was 65.4 Hz and the string was assumed ideal for simplicity so that the natural frequencies are harmonic. However, a real string would be modelled with equal ease by using the corresponding inharmonic modes. The string was modeled using a modal basis of 80 modes and an average modal damping of 0.1% was used for all modes. The friction parameters were $\mu_S = 0.4$, $\mu_D = 0.2$ and $C = 5$ and the bowing contact point was 4 cm from the bridge. The string/body coupling parameters were $K_{BS} = 10^8$ N.m^{-1}. For the finger model, values of $W_f = 1$ cm, $K_{FS} = 10^5$ N.m^{-1} and $C_{FS} = 10$ N.s.m^{-1} were used. For simplicity, the instrument body was modeled using a single body mode, experimentally identified at 195.9 Hz with a modal damping value of about 1.3%. Note that including a multimodal basis for the instrument body can be easily done since a full modal formulation of the problem

is employed in our model. Because of the explicit nature of the integration algorithm used, a small time-step of 10^{-6}s was adopted.

As a first example, Figure 1 shows the time-domain response of the bridge obtained for a slow increasing ramp in bow velocity ($0.01 \leq v_b \leq 0.1$ m/s, T_{cal}=10 s) and a fixed bow force (F_N=0.5 N) during a wolf (x_f=0.368 m). Results show

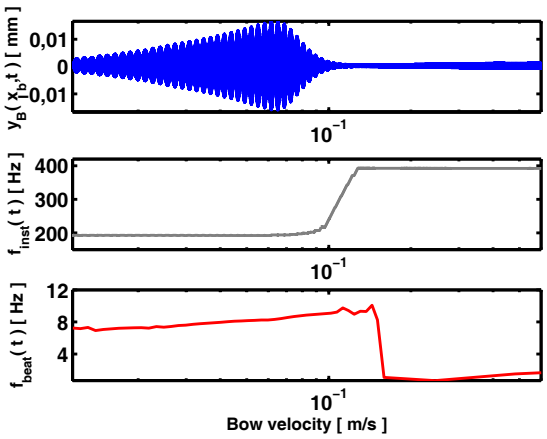

Figure 1: Simulation of a cello string bowed at the wolf note position, for an exponential ramp in bow velocity. Time-domain bridge response (up), instantaneous frequency (middle) and time-varying beating frequency (above). $0.01 \leq v_b \leq 0.1$ m/s, F_N=0.5 N.

clearly that a pronounced wolf is excited for the lower bow velocity values as attested by the increase of the amplitude response and the presence of beats. For higher bow velocities, the wolf note collapses and a higher-order regime of low amplitude settles, dominated by the second modal frequencies as seen from the computed time-varying playing frequency. It is interesting to note that the model thus captures some essential characterisitcs of wolf notes, since such behaviour is often encountered in playing experience. Of particular interest is the increase in the wolf note beating frequency (estimated using a zero-cross counting technique from the amplitude of the Hilbert transform) as the bow velocity increases. In practice, it suggests that the suppression of the beats can be provided by adopting a slower bow velocity.

The second example concerns the simulation of a wolf note as the bow force is increased ($0.01 \leq F_N \leq 10$ N, T_{cal}=10 s) for a fixed bow velocity (v_b=0.02 m/s, x_f = 0.368 m). Results are shown in Figure 2. For low force values, a low-amplitude higher-order regime is excited, dominated by the second modal frequency, as seen from the plots of the bridge response and of the instantaneous frequency. When the bow force becomes higher, it gives way in turn to successive oscillating regimes, respectively a wolf note regime, a Helmholtz regime and finally a raucous regime as supported by the dominant frequency variations. Particularly, one recognizes the flattening increase of the played note with bow force when the bow force exceeds a threshold value as described in [5]. However, identifying the wolf note region is not as evident as in the first case. To overcome this problem, we compute the standard deviations of the bridge response and of its envelope, estimated by Hilbert transform. Comparing these information and using the time-varying frequency and time-history bridge response, a range of bow force for which a

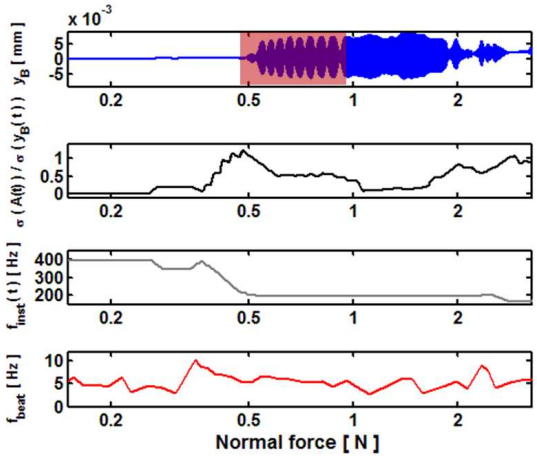

Figure 2: Simulation of a cello string bowed at the wolf note position, for an exponential sweep in bow normal force. v_b = 0.02 N. From top to bottom: time-domain bridge response; relative standard deviation between the bridge envelope and the bridge response; time-varying frequency; beating frequency.

wolf occurs can be estimated (in red in the time-history bridge response). Then, looking at the lower plot in Figure 2, one can note a small decrease of the beating frequency during the wolf, from 7 to 5 Hz while the bow force increases of about 4/3. Such dependence of the beating frequency with the bow force has already been discussed in [5].

3 Linear analysis

Despite the strong nonlinearity coming from the frictional force, attention is now focused on the linearized string/body coupled model which provides an appropriate framework to study system instabilities as usually done for friction-induced squeal problems [12]. The dynamic equilibrium state is a steady sliding state which means that the operating point of the linearized system does not include the very steep part of the friction curve (see Ref. [5, 13, 7]).

3.1 Modal formulation

Looking for solutions in the form of Eq. (4) for the linear model , the string displacement, velocity and acceleration are now written as:

$$y_s(x,t) = \bar{y}_s(x) + \hat{y}_s(x,t) = \sum_{n=1}^{N_s} \bar{q}_n \varphi_n(x) + \sum_{n=1}^{N_s} \hat{q}_n(t)\varphi_n(x) \tag{10}$$

$$\dot{y}_s(x,t) = \dot{\hat{y}}_s(x,t) = \sum_{n=1}^{N_s} \dot{\hat{q}}_n(t)\varphi_n(x) \tag{11}$$

$$\ddot{y}_s(x,t) = \ddot{\hat{y}}_s(x,t) = \sum_{n=1}^{N_s} \ddot{\hat{q}}_n(t)\varphi_n(x) \tag{12}$$

noting a bar and a hat for the steady deformed state and small-amplitude oscillating quantities respectively. Since a small perturbation of the steady sliding state will be influenced by the friction curve locally, the non-linear frictional force can be linearized around the associated mean string velocity. The Taylor-serie expansion of Eq. (6) for $\dot{y}_s(x_c,t) \ll$

v_{bow} gives:

$$\mu_d(t) \simeq \mu_D + (\mu_S - \mu_D)e^{-Cv_b}[1 + C\dot{y}_s(x_c,t)] \quad (13)$$

and the frictional force becomes in the linearized model

$$f_c(t) \simeq \bar{f}_c + \hat{f}_c(t) \quad (14)$$

where $\bar{f}_c$ and $\hat{f}_c(t)$ are the static and small-amplitude oscillating force components given by:

$$\begin{aligned} \bar{f}_c &= F_N\,[\,\mu_D + (\mu_S - \mu_D)e^{-Cv_b}\,] \\ \hat{f}_c(t) &= A\,\dot{y}_s(x_c,t) \end{aligned} \quad (15)$$

denoting A a control parameter which encapsulates all the relevant parameters of the friction model:

$$A = F_N\,(\mu_S - \mu_D)\,C\,e^{-Cv_b} \quad (16)$$

By replacing (10), (11) and (12) in Eqs.(2), (7), (8) and (15), one obtains a set of equations for the static modal amplitudes ($\bar{q}_n$ and $\bar{q}_m$) and a set of equations for the vibratory modal amplitudes ($\hat{q}_n$ and $\hat{q}_m$). The former set plays no role in the dynamics of the perturbations analysis, as the zero-order solution only represents a mean deformed state due to the static force $\bar{f}_c$. However, the latter set provides information about the system stability and how the linearized sliding state will subsequently evolves. The first-order linearized system is written as:

$$[\mathbf{M}]\{\ddot{\hat{Q}}\} + [\mathbf{C}]\{\dot{\hat{Q}}\} + [\mathbf{K}]\{\hat{Q}\} = \{\hat{F}_c\} + \{\hat{F}_b\} + \sum_{j=1}^{3}\{\hat{F}_{f_j}\} \quad (17)$$

where $[\mathbf{M}]$, $[\mathbf{C}]$ and $[\mathbf{K}]$ are diagonal matrices pertaining to the coupled system modal parameters and $\{\hat{Q}\} = \{\{\hat{Q}_s\}\,\{\hat{Q}_b\}\}^T$ is a vector for the small-amplitude modal responses given by:

$$[\mathbf{M}] = \begin{bmatrix} \mathbf{M}_s & 0 \\ 0 & \mathbf{M}_b \end{bmatrix},\ [\mathbf{C}] = \begin{bmatrix} \mathbf{C}_s & 0 \\ 0 & \mathbf{C}_b \end{bmatrix},\ [\mathbf{K}] = \begin{bmatrix} \mathbf{K}_s & 0 \\ 0 & \mathbf{K}_b \end{bmatrix}$$

The right-hand-side terms of Eq.(17) stem from the modal projections of the linearized force field provided by the friction force, the string/body coupling and the finger/string interaction with the following expressions:

$$\{\hat{F}_c\} = \begin{bmatrix} A\boldsymbol{\Phi}(x_c) & 0 \\ 0 & 0 \end{bmatrix}\{\dot{\hat{Q}}\} \quad (18)$$

$$\begin{aligned} \{\hat{F}_b\} = &-K_{BS}\begin{bmatrix} \boldsymbol{\Phi}_{SS}(x_b) & \boldsymbol{\Phi}_{SB}(x_b) \\ \boldsymbol{\Phi}_{BS}(x_b) & \boldsymbol{\Phi}_{BB}(x_b) \end{bmatrix}\{\hat{Q}\} \\ &- C_{BS}\begin{bmatrix} \boldsymbol{\Phi}_{SS}(x_b) & \boldsymbol{\Phi}_{SB}(x_b) \\ \boldsymbol{\Phi}_{BS}(x_b) & \boldsymbol{\Phi}_{BB}(x_b) \end{bmatrix}\{\dot{\hat{Q}}\} \end{aligned} \quad (19)$$

$$\begin{aligned} \{\hat{F}_{f_j}\} = &-K_{BS}\begin{bmatrix} \boldsymbol{\Phi}_{FS}(x_{f_j}) & 0 \\ 0 & 0 \end{bmatrix}\{\hat{Q}\} \\ &- C_{BS}\begin{bmatrix} \boldsymbol{\Phi}_{FS}(x_{f_j}) & 0 \\ 0 & 0 \end{bmatrix}\{\dot{\hat{Q}}\} \end{aligned} \quad (20)$$

with the coupling matrices

$$\begin{aligned} \boldsymbol{\Phi}(x_c) &= \{\varphi_n(x_c)\}\{\varphi_n(x_c)\}^T \quad \boldsymbol{\Phi}_{FS}(x_{f_j}) = \{\varphi_n(x_{f_j})\}\{\varphi_n(x_{f_j})\}^T \\ \boldsymbol{\Phi}_{SS}(x_b) &= \{\varphi_n(x_b)\}\{\varphi_n(x_b)\}^T \quad \boldsymbol{\Phi}_{SB}(x_b) = -\{\varphi_n(x_b)\}\{\phi_p(x_b)\}^T \\ \boldsymbol{\Phi}_{BS}(x_b) &= -\{\phi_p(x_b)\}\{\varphi_n(x_b)\}^T \quad \boldsymbol{\Phi}_{BB}(x_b) = \{\phi_p(x_b)\}\{\phi_p(x_b)\}^T \end{aligned}$$

By assuming harmonic solutions, Eq.(17) leads to a standard eigenvalue problem. The eigenvalues $\lambda_n = \sigma_n \pm i\tilde{\omega}_n$ computed are in general complex and provide, apart the (damped) modal frequencies $\tilde{\omega}_n = \Im m(\lambda_n)$, the modal dissipation values $\zeta_n = \Re e(\lambda_n)/|\lambda_n|$ which determine the system behaviour before nonlinear effects take control. Particularly, eigenvalues with a positive real part are characteristics of an unstable state which will ultimately lead to self-sustained vibrations. In particular, we expect to detect variations in the modal frequencies of two unstable closely spaced modes - modes which may be responsible for the wolf - by studying the evolution of the eigenvalues as function of the input control parameters.

3.2 Modal behaviour of the string-body coupled system

To fix idea, Figure 3 shows a typical stability plot for the first modes of the coupled system as a function of the excitation control parameter A. A low-E (f=65.4 Hz) note is played, the green colour stands for stability and the red colour for instability. As expected from Eq.(16) and illustrated in Figure 3, the parameter A clearly influences the stable/unstable behaviour of the system coupled modes. Globally, it can be observed that many modes - those of the active length of the string with harmonic series frequencies - become unstable as A increases whereas other modes - those to the bridge-tailpiece distance - remain stable. Interestingly, Figure 3 readily gives an alternative interpretation of the Helmholtz motion, in terms of modes, instead of the well-known text-book description involving a Helmholtz corner circulating backward and forwards along the string [13]. It is then tempting to link these results to the player's experience. For instance, the fact that higher modes loose their stability before the fundamental mode might be related to the so-called *surface sound* when the bow force is below the minimum bow force as defined by Schelleng [14]. Further demonstrative cases are given in Ref. [8].

The dependence of the wolf note beating frequency with the input control parameters is now considered with the help of the results plotted in Figure 4. As can be seen, the linear approach predicts regions of instability for two closely space

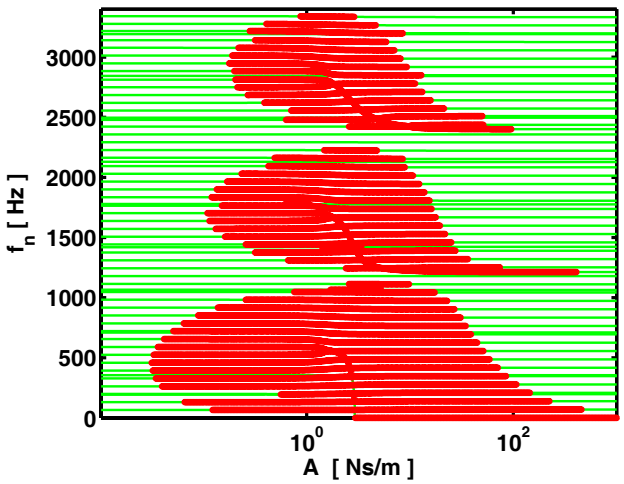

Figure 3: Stability plot as function of the coefficient A. Green: stability; Red: instability.

coupled modes in the neighbourhood of the body resonance, when the bow force or the the bow velocity vary. As suggested in [9], such behaviour can be interpreted as a plausible occurence of a wolf note regime. To go further and to support the idea that something can be gained by a linear analysis, a more interesting situation is revealed when we look at the frequency evolution of those two unstable modes as the input parameters vary during a wolf. Figure 4 indicates that the frequency separation of the two unstable modes decreases as the bow normal force increases. Reminding that the beat frequency is equal to the absolute value of the difference in frequency of the two modes, this in turn leads to a decrease of the beat pulsation, a tendency observed in nonlinear computations (see Figure 2). Interestingly, the well-known fact that pressing harder with the bow can ultimately suppress the beating in the wolf note is also apparent in the present linear analysis. Actually, Figure 4 predicts the stabilization of one of the two unstable coupled modes when the normal force exceeds a threshold value, which is the effect described by Raman [6].

Other interesting aspect is revealed considering the influence of the bow velocity. Figure 4 shows an increase of the frequency difference between the two unstable modes as the bow velocity is increased. In other words, the beating frequency of the wolf grows with the bow velocity. This is precisely the behaviour provided by our nonlinear time-domain computations (see Figure 1) and experienced on our instrument. To make a critical comparison with the nonlinear computations, Figure 4 suggests an upward frequency shift of the unstable mode as the normal force increases although the *flattening effect* is undoubtedly a physical reality [5]. Such unrealistic result does not imply that our linear predictions are seriously unrealistic. It is well-know that an hysteresis occurs during the transition from slipping to sticking [5, 13], an effect which is intrinsically due to the severe nonlinearity of the friction force. These variations are, obviously, something that the linear approach cannot predict.

Finally, Figure 5 represents the stability plots of the two coupled modes as a function of the bow normal force and velocity. According to our linearized analysis, it is apparent that a range of bow force and bow velocity exists for which the two modes are unstable. It is then instructive to compare the linear predictions with the results presented in Figure 6, stemming from nonlinear computations at discrete bow force values for an increase of bow velocity. Even if the agreement is not expected to be very precise since there are many missing factors in the linear approach, the linear analysis predicts instability of a pair of coupled modes in approximately the same ranges as the nonlinear computations.

Overall, these results support the fact that a linear approach captures some essential characteristics of wolf note regime and can thus provide some interesting information with a lower-expensive computer cost than nonlinear computations.

4 Conclusions

In this paper, a linearized analysis of the string/body coupled system dynamics subjected to the highly non-linear bow/string friction force mechanism was performed. Obviously, the linear approach does not directly provide a precise information on the nonlinear self-excited regimes. Nevertheless, this paper presents several examples showing that a linearized approach of this particular nonlinear problem can be instructive in predicting the gross features of the nonlinear regimes. In particular, the interesting phenomenon of the dependence of the wolf beating frequency with the input parameters can be understood. As pointed out by Inacio et al. [7], these results also suggest insights on the mechanism through which musicians usually try to control wolf-notes.

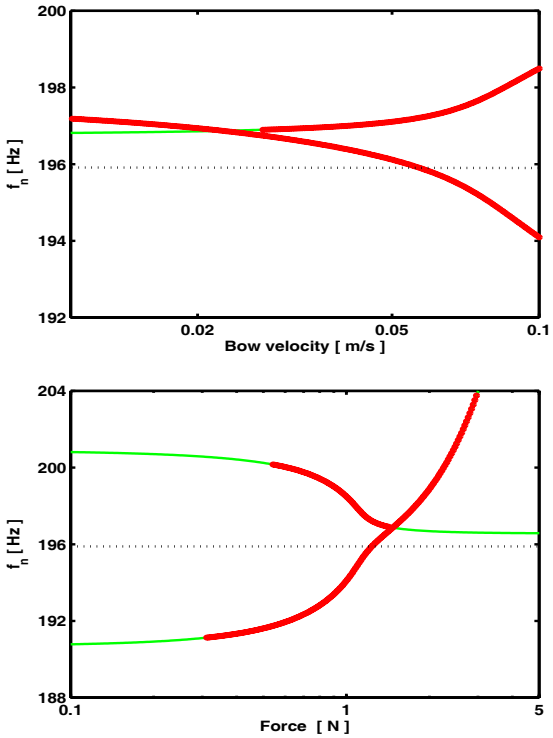

Figure 4: Stability plots of the two coupled modes which may be responsible for the wolf. Up: as function of the bow velocity; Down: as a function of the bow force. Green: stability; Red: instability. Dot: uncoupled body resonance frequency.

Acknowledgments

This work has been endorsed by the Portuguese Fundação para a Ciência e Tecnologia (FCT) under the project reference PTDC/FIS/103306/2008.

References

[1] J. C. Schelleng. The violin as a circuit. *J. Acoust. Soc. Am.*, 35(3):326–338, 1963.

[2] J. Woodhouse. On the playability of violins. parts II: Minimum bow force and transients. *Acustica*, 78:137–153, 1993.

[3] E. Gough. The resonant response of a violin g-string and the excitation of the wolf note. *Acustica*, 44:113–123, 1980.

[4] M. E. McIntyre and J. Woodhouse. On the fundamentals of bowed-string dynamics. *Acustica*, 43:93–108, 1979.

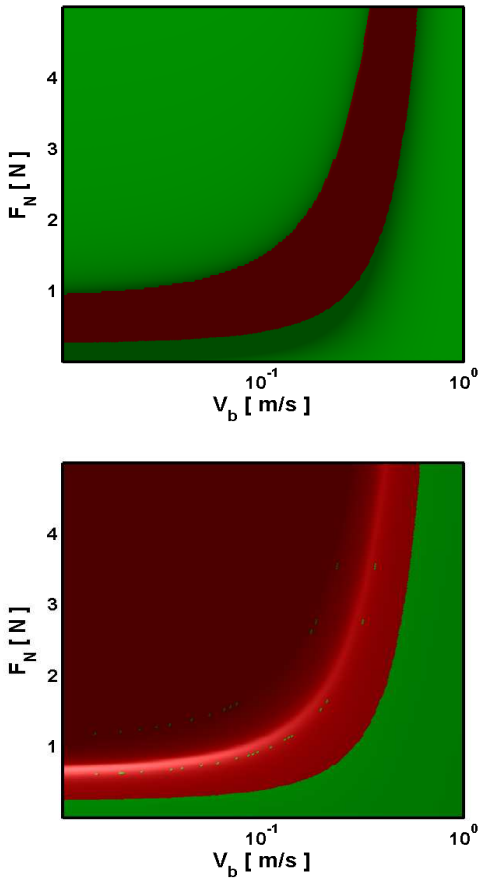

Figure 5: Stability plots of the two coupled modes which may be responsible for the wolf. Green: stability; Red: instability.

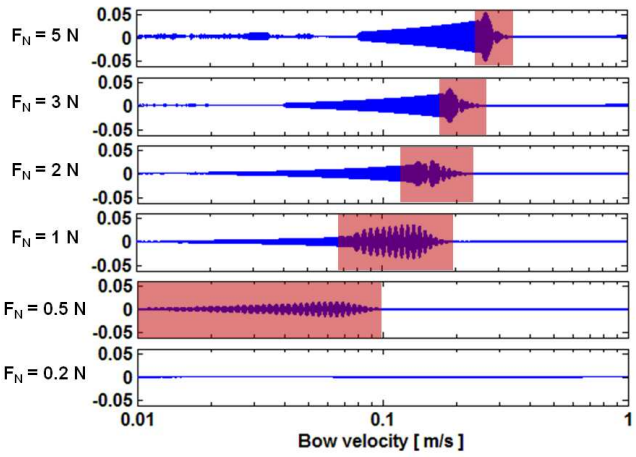

Figure 6: Simulation of a cello string bowed at the wolf note position, for an exponential ramp in bow velocity for discrete values of bow force. Time-domain bridge response. Wolf-note regime appears in transparent red.

[5] M. E. McIntyre, R. T. Schumacher, and J. Woodhouse. On the oscillations of musical instruments. *J. Acoust. Soc. Am.*, 74(5):1325–1345, 1983.

[6] C. V. Raman. Wolf-note in bowed string instruments. *Philos. Mag.*, 32:391, 1916.

[7] O. Inácio, J. Antunes, and M.C.M. Wright. Computational modelling of string-body interaction for the violin family and simulation of wolf notes. *J. Sound. Vib.*, 310:260–286, 2007.

[8] O. Inácio and J. Antunes. A linearized modal analysis of the bowed string. In *Proceedings of the ICA Conference*, 2007.

[9] V. Debut, J. Antunes, and O. Inacio. A linearized modal approach for predicting wolf notes. In *ICSV2011 proceedings*, Rio de Janeiro, 2011.

[10] V. Debut, O. Inácio, J. Antunes, and T. Dumas. Modelling and experiments on string/body coupling and the effectiveness of a cello wolf-killing device. In *ISMA2010 proceedings*, Katoomba, 2010.

[11] J.N. Juang. *Applied system identification*. Prentice-Hall PTR, 1994.

[12] H. Ouyang and W. Nack. Numerical analysis of automotive disc brake squeal: a review. *Int. J. Vehicule Noise and Vibration*, 1:207–231, 2005.

[13] J. Woodhouse. Self-sustained musical oscillators. In A. Hirschberg/ J. Kergomard/ G. Weinreich, editor, *Mechanics of musical instruments*, volume 335 of *CISM Courses and Lectures*, pages 185–228. Springer-Verlag, Wien- New York, 1995.

[14] J. C. Schelleng. The bowed sring and the player. *J. Acoust. Soc. Am.*, 53:26–41, 1973.